Evaluation of a QT Adaptation Time Estimator for ECG Exercise Stress Test in Controlled Simulation

Cristina Pérez[1], Esther Pueyo[1,2], Juan Pablo Martínez[1,2], Leif Sörnmo[3], Pablo Laguna[1,2]

[1] BSICoS Group, I3A, IIS Aragón, University of Zaragoza, Zaragoza, Spain
[2] CIBER-Bioengineering, Biomaterials and Nanomedicine (CIBER BBN), Madrid, Spain
[3] Department of Biomedical Engineering, Lund University, Sweden

Abstract

Slowed adaptation of the QT interval to sudden abrupt heart rate (HR) changes has been identified as a marker of ventricular arrhythmic risk. However, abrupt HR changes are difficult to induce in patients. Quantifying the QT adaptation time in gradual HR changes, as observed in ECGs recording during an exercise stress test, has been recently proposed. The time lag between the QT series and an instantaneous memoryless HR-dependent QT series along stress test was computed as QT memory. Here, this method was evaluated in a control scenario using simulated exercise stress test ECG signals presenting different QT adaptation times. The method robustness was studied by contaminating the ECGs with muscular noise (MN) signals with different Signal-to-Noise ratio (SNR) values, either synthetic or extracted from real recordings. We found that delineation of the T-wave end point in the first transformed lead from Periodic Component Analysis offers the best performance for low SNR. Moreover, we confirmed that the estimator provides an unbiased estimate of the QT memory introduced in the simulations for the studied range of SNR values (25 to 50 dB).

1. Introduction

Increased spatio-temporal heterogeneity in ventricular repolarization is related to cardiac instabilities that could lead to ventricular arrhythmias and sudden cardiac death (SCD) [1]. The adaptation time of the QT interval to sudden changes in heart rate (HR) has been identified as a marker for arrhythmic risk [2]. However, abrupt HR changes are not always easily observed in Holter recordings. Therefore, we proposed to estimate the QT memory as the lag between the QT series and an instantaneous memoryless HR-dependent QT series from gradual HR changes, as those that can be observed during an exercise stress test (EST) following a ramp-like shape. The delay was evaluated independently in the exercise and in the re-

covery periods and showed values of QT adaptation dynamics in the same ranges as those computed following abrupt HR changes [3]. However, the robustness and precision of the algorithm can not be evaluated from real data where the "truth" is not available.

In this study, we generated simulated ECGs whose RR dynamics come from real data recorded during an EST [4]. The RR-QT relationship included a non-linear part and the QT memory part in which the QT adaptation time was an input parameter. ECGs were contaminated with either synthetic or real muscular noise (MN) signals with selected Signal-to-Noise Ratio (SNR) values. The study aims were: (1) to evaluate the T-wave end point (T_e) delineation by different spatial lead transformation aiming to emphasize the T-wave; and (2) to study the robustness and precision of the QT adaptation time estimator by computing the delay between the QT series and an instantaneous memoryless HR-dependent QT series in ECGs with different SNR.

2. Methods

2.1. Dataset

Simulated ECGs with different QT adaptation times (τ) were computed with a predefined RR series pattern from an EST, but modified so that the stress peak was kept in the same RR value for 10 minutes to facilitate convergence to a stationary QT-RR relation before recovery started. Ten ECGs were produced for each selected τ, taken from 10 to 50 s, in steps of 10 s, resulting in a total of 50 clean simulated ECGs, containing the 8-standard leads V1-V6, I and II, with a sampling frequency of 1000 Hz. An evolved version [4] of the simulator in [5] was used to generate these signals. The simulator's user-defined parameters are given in Table 1. Synthetic or real MN signal with different Signal-to-Noise Ratio (SNR) was added to the clean simulated ECGs.

Zero-mean synthetic MN signals were created by the model defined in [4], which is constant in resting periods

Table 1: User-defined parameters in the ECG simulator.

	Parameter	User value
Period duration (min)	Basal onset	10
	Exercise ramp	*
	Peak	10
	Recovery ramp	*
	Basal end	10
HR (bpm)	Basal onset	80
	Peak	165
	Basal end	95
Respiratory frequency (Hz)	Basal onset	0.25
	Peak	0.7
	Basal end	0.3

*Duration of both exercise and recovery ramps were defined using length and peak position information of 10 available real noise signals extracted from signals recording during an EST [6].

and linearly increased in the exercise stage or decreased in the recovery stage. The MN noise variance at the exercise peak was selected to be four times the variance at the beginning (basal onset) and was selected according to the desired SNR:

$$\text{SNR}_l = 20 \log_{10} \left(\frac{\text{A}_{\text{QRS},l}}{\text{RMS}_{\text{noise},l}} \right) \quad (1)$$

where $\text{A}_{\text{QRS},l}$ is the peak-to-peak amplitude of the ensemble-averaged QRS of lead l (determined in a 100-ms interval centered around R-peak, $n_{\text{QRS},k}$, of the k-th beat) [6, 7]. The entire MN signal was rescaled so that its RMS value in a window of 60 s at the exercise peak was $\text{RMS}_{\text{noise},l}$.

Real MN signals were extracted from recordings during EST [6] using a bandpass filter whose lower and upper cut-off frequencies are 10 and 200 Hz, respectively. To scale real MN signals to a desired SNR, a factor was calculated using the RMS information of the 60 s around the exercise peak of real MN signal and the $\text{RMS}_{\text{noise},l}$ value from eq (1). Independent MN signals were added to each of the leads, both for synthetic and real MN signals.

The SNR values defined, for both types of MN, were 25, 30, 35, 40, and 50 dB. Thus, the dataset was composed of 500 ECGs contaminated with noise.

2.2. T-wave end delineation performance

We assessed the accuracy of delineating the T-wave end, T_e, using a multi-lead (MLead) delineation strategy as well as by delineating the first-transformed lead obtained with different Lead Space Reduction (LSR) techniques.

ECGs were filtered before delineation. First, high-frequency noise and artifacts were attenuated by using a 6th-order Butterworth low-pass filter, with a cut-off frequency of 50 Hz, implemented in a forward-backward version. Afterwards, baseline wander was attenuated using cubic spline interpolation.

Different methods based on two LSR techniques, Periodic Component Analysis (πCA)[8] and Principal Component Analysis (PCA) [9] were proposed to obtain a transformed lead where T-waves were emphasized. Subsequently, the lead was delineated [10] to compute T_e [11]. The different versions of the methods based on the two mentioned LSR techniques are:

- **πCA:** or GπCA$_1$, The transformation was learned in each signal window of 150 seconds, recalculating the transform $\mathbf{\Psi}$ matrix in each window, for beat periodicity $P = 1$.
- **GπCA$_3$:** The transformation was learned in each window of 150 seconds recalculating $\mathbf{\Psi}$ matrix, with $P = 3$.
- **πCA$_o$:** GπCA$_{1,o}$, where the $\mathbf{\Psi}$ matrix was estimated once using the first 150 seconds at the onset of the signal and $P = 1$, and then the same transformation $\mathbf{\Psi}$ was applied to the rest of the signal.
- **GπCA$_{3,o}$:** The $\mathbf{\Psi}$ matrix was estimated once using the information at the signal onset, in the first 150 seconds, and then applied to the complete signal, with $P = 3$.
- **PCA:** PCA technique where transform $\mathbf{\Psi}$ matrix was re-estimated in each window of 150 seconds.
- **PCA$_o$:** PCA technique where $\mathbf{\Psi}$ matrix was estimated once at the signal onset, using the information of the first 150 seconds, and then applied to the complete signal.

Delineation marks of each k-th beat of the simulated ECGs contaminated with MN with an SNR = 50dB, $T_{e,k}^r$, were used as reference values to study delineation performance at higher noise levels. The delineation error, ϵ, was calculated as:

$$\epsilon = \sqrt{\left(\frac{1}{K} \sum_{k=1}^{K} \left(T_{e,k}^r - T_{e,k} \right)^2 \right)} \quad (2)$$

where K is the number of beats whose T_e is defined.

2.3. Performance of QT adaptation time estimator

The time lag between the QT series $d_{\text{QT}}(n)$ and an instantaneous memoryless HR-dependent QT series $d_{\text{QT}}^i(n)$ reflects the QT adaptation time when HR gradually changes following a ramp-like shape. The $d_{\text{QT}}^i(n)$ series was obtained by a hyperbolic regression model accounting for its dependency with RR series $d_{\text{RR}}(n)$[3], so both RR and QT series were needed to evaluate the delay.

Both the R-wave and QRS onset (QRS$_o$) points were obtained by delineating each lead [10] and subsequently a multi-lead strategy was applied to assign a unique mark to a beat. To compute T_e, the first transformed lead of the GπCA$_{3,o}$ was delineated [3].

The time lag between $d_{\text{QT}}^i(n)$ and $d_{\text{QT}}(n)$ was estimated in the exercise ramp, $\hat{\tau}_e$, and in the recovery ramp, $\hat{\tau}_r$, sep-

arately, using a least squares estimator: [3].

$$\hat{\tau} = \arg\min_{\tau} \sum_{n=n_o}^{n_e} \left(d_{\mathrm{QT}}^i(n) - d_{\mathrm{QT}}(n+\tau) \right)^2; \ \tau \in \{-I, ..., I\},$$
(3)

with I representing the plausible range of values for τ, and n_o and n_e the onset and end of the ramps, respectively.

In a previous study [3], an automatic algorithm was developed to determine n_o and n_e based on the the sum of (3). The onset of the exercise area was defined as the intercept between the flat basal area before the exercise and the linear decreasing $d_{\mathrm{QT}}^i(n)$ ramp at exercise. The same idea was employed to define the end of the recovery area using now the recovery and the basal area after it. Both the end of the exercise and the onset of the recovery were established at 55% of the total ramp $d_{\mathrm{QT}}^i(n)$ excursion, implying being away from the exercise peak, see [3].

3.   Results and Discussion

Fig. 1 shows the mean and standard deviations of the delineation errors, ϵ, for each delineation method, SNR value, and noise type. It can be observed from Fig.1a that the lower the SNR, the better any πCA technique performances. When the ECGs were contaminated with synthetic MN, GπCA$_{3,o}$ reached $5.97 \pm 3.32, 3.71 \pm 2.09$, 2.67 ± 1.79 and 1.85 ± 1.00 ms for SNR = 25, 30, 35 and 40 dB, respectively. PCA methods showed the lowest error when the SNR was high, although this error was not far away from the error obtained with any of the πCA methods ($6.35 \pm 3.78, 3.56 \pm 2.07, 2.00 \pm 0.98$ and 1.19 ± 1.00 ms for SNR = 25, 30, 35 and 40 dB, respectively, with PCA$_o$). The Mlead strategy exhibited the worst delineation performance except for 25 dB ($6.09 \pm 2.26, 4.74 \pm 1.70$, 3.67 ± 1.39 and 2.89 ± 1.42 ms for SNR = 25, 30, 35, and 40 dB, respectively). A less clear tendency was observed in ϵ when ECGs were contaminated with real MN. The lower the SNR, the better the performance of πCA. In cases with SNR values lower than 25 dB, πCA outperformed the other delineation strategies for real noise and GπCA$_{3,o}$ for synthetic noise. These results are in agreement with our previous study [11] where the beat-to-beat variability over the real QT series was used as a surrogate of T_e delineation performance. When the SNR was equal to 25 dB, the algorithm was not able to delineate 33% of the T-wave end points using the Mlead strategy, while the algorithm was able to delineate around 99% of the T-wave end points using LSR methods. Since we found T_e delineation critical when the SNR value was lower than 25 dB, the first transformed lead obtained with GπCA$_{3,o}$ method was selected to compute the T_e delineation based on the above described results.

The mean and standard deviation of the estimated delays in exercise, $\hat{\tau}_e$, and in recovery, $\hat{\tau}_r$, were computed for
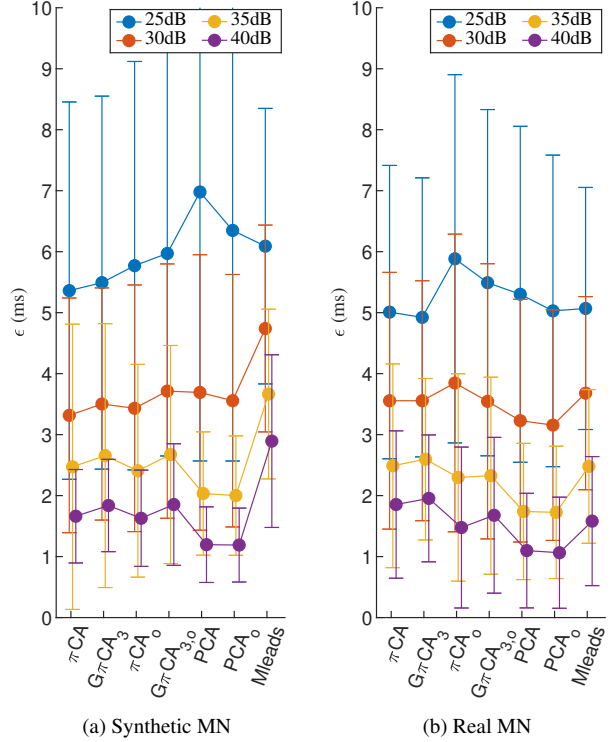

(a) Synthetic MN   (b) Real MN

Figure 1: Mean and standard deviation of the delineation error, ϵ, for each delineation method, SNR and noise type.

ECGs with different QT adaptation times, SNR values and noise types, and are presented in Fig 2. We can observe similar results when $\hat{\tau}_e$ was calculated from ECGs contaminated with synthetic or real MN. The mean estimated adaptation values were slightly biased, with the estimated times being higher than the simulated ones. In the recovery, we observed a lower influence of the SNR value when the QT adaptation time was shorter. Moreover, $\hat{\tau}_r$ values were biased, but in this case the estimated times were lower than the simulated ones. The bias did not exceed 20% in any case. In general, the standard deviation was higher for lower SNR.

4.   Conclusions

A study on simulated-exercise-stress-test ECGs with a predefined QT-RR relationship and well-defined muscular noise levels was performed. We confirmed that the lower the SNR, the more advantage can be taken from πCA-based methods for T-wave end delineation. Besides, our study confirms that the estimated time lag between the QT series and an instantaneous memoryless HR-dependent QT series is minimally biased with respect to the underlying QT adaption time imposed in the simulated ECGs, with this holding true for the simulated range of SNR values (25 to 50 dB).
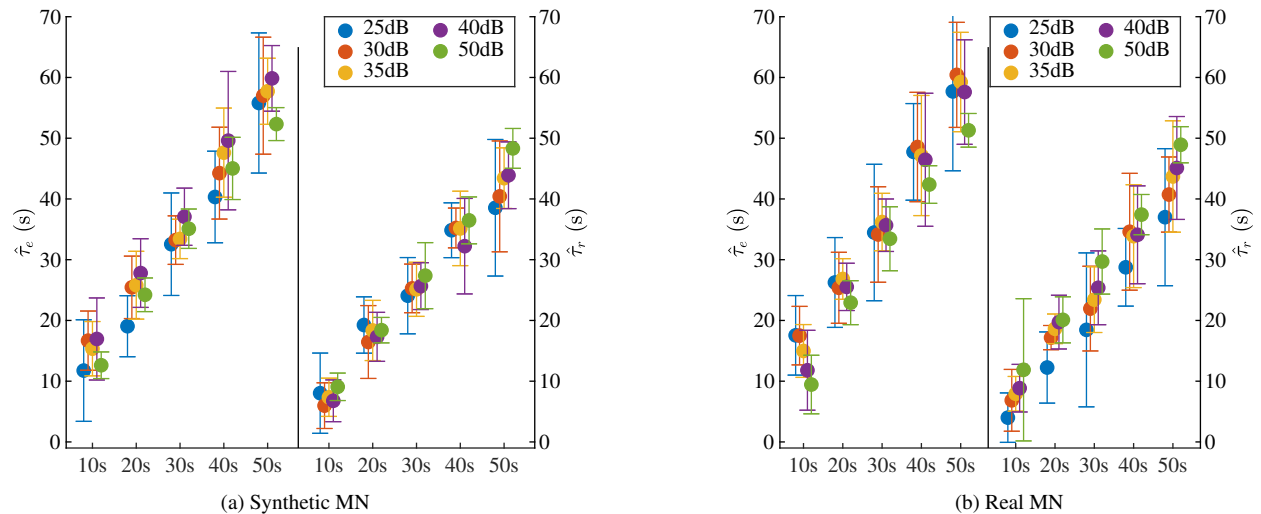
(a) Synthetic MN   (b) Real MN

Figure 2: Mean and standard deviation of the estimated delays in exercise, $\hat{\tau}_e$, and in recovery, $\hat{\tau}_r$, computed for ECGs with different QT adaptation times, SNR values and noise types.

Acknowledgments

References

[1] Arteyeva NV. Dispersion of ventricular repolarization: Temporal and spatial. World Journal of Cardiology 2020; 12(9):437.

[2] Pueyo E, Smetana P, Caminal P, De Luna AB, Malik M, Laguna P. Characterization of QT interval adaptation to RR interval changes and its use as a risk-stratifier of arrhythmic mortality in amiodarone-treated survivors of acute myocardial infarction. IEEE Transactions on Biomedical Engineering 2004;51(9).

[3] Pérez C, Pueyo E, Viik J, Martínez JP, Laguna Pa. QT interval time lag in response to heart rate changes during stress test for coronary artery disease diagnosis. Biomedical Signal Processing and Control ;86(105056).

[4] Bachi L, Halvaei H, Pérez C, Martín-Yebra A, Petrénas A, Johnson L, Marozas V, Martínez JP, Pueyo E, Stridh M, Laguna P, Sörnmo L. ECG modeling for simulation of arrhythmias in time-varying conditions. IEEE Transactions on Biomedical Engineering 2023;In press(v).

[5] Petrenas A, Marozas V, Sološenko A, Kubilius R, Skibarkiene J, Oster J, Sörnmo L. Electrocardiogram modeling during paroxysmal atrial fibrillation: application to the detection of brief episodes. Physiological Measurement 2017;38(11):2058.

[6] Bailón R, Sornmo L, Laguna P. A robust method for ecg-based estimation of the respiratory frequency during stress testing. IEEE transactions on biomedical engineering 2006; 53(7):1273–1285.

[7] Martín-Yebra A, Sörnmo L, Laguna P. QT interval adaptation to heart rate changes in atrial fibrillation as a predictor of sudden cardiac death. IEEE Transactions on Biomedical Engineering 2022;69(10):3109–3118.

[8] Sameni R, Jutten C, Shamsollahi MB. Multichannel electrocardiogram decomposition using periodic component analysis. IEEE transactions on biomedical engineering 2008;55(8):1935–1940.

[9] Castells F, Laguna P, Sörnmo L, Bollmann A, Roig JM. Principal component analysis in ECG signal processing. EURASIP Journal on Advances in Signal Processing 2007; 2007:1–21.

[10] Martínez JP, Almeida R, Olmos S, Laguna P. A wavelet-based ECG delineator: evaluation on standard databases. IEEE Transactions on biomedical engineering 2004;51(4).

[11] Pérez C, Martín-Yebra A, Viik J, Martínez JP, Pueyo E, Laguna P. Eigenvector-based spatial ECG filtering improves QT delineation in stress test recordings. In 2021 55th Asilomar Conference on Signals, Systems, and Computers. IEEE, 2021; 261–264.

Address for correspondence:

Cristina Pérez Martínez (cperez@unizar.es)
Ed. Ada Byron, C/María de Luna 1, 50018 Zaragoza, Spain